

# Exact diagrammatic approach for dimer-dimer scattering and bound states of three and four resonantly interacting particles.

I.V. Brodsky and M.Yu. Kagan\*

*P.L. Kapitza Institute for Physical Problems, Kosygin street 2, Moscow, Russia, 119334*

A.V. Klaptsov

*Russian Research Centre "Kurchatov Institute", Kurchatov square 1, Moscow, Russia, 123182*

R. Combescot and X. Leyronas

*Laboratoire de Physique Statistique, Ecole Normale Supérieure,  
24 rue Lhomond, 75231 Paris Cedex 05, France*

(Dated: July 3, 2018)

We present an exact diagrammatic approach for the dimer-dimer scattering problem in two or three spatial dimensions, within the resonance approximation where these dimers are in a weakly bound resonant state. This approach is first applied to the calculation of the dimer-dimer scattering length  $a_B$  in three spatial dimensions, for dimers made of two fermions in a spin-singlet state, with corresponding scattering length  $a_F$  and the already known result  $a_B = 0.60 a_F$  is recovered exactly. Then we make use of our approach to obtain new results in two spatial dimensions for fermions as well as for bosons. Specifically, we calculate bound state energies for three  $bbb$  and four  $bbbb$  resonantly interacting bosons in two dimensions. We consider also the case of resonant interaction between fermions and bosons and we obtain the exact bound state energies of two bosons plus one fermion  $bbf$ , two bosons plus two fermions  $bf_\uparrow bf_\downarrow$ , and three bosons plus one fermion  $bbbf$ .

PACS numbers: 03.75.Ss, 05.30.Fk, 21.45.+v, 31.15.-p

Keywords:

## I. INTRODUCTION

Following the experimental realization of the Bose-Einstein condensation in ultracold bosonic gases, together with its intensive study, the physics of ultracold Fermi gases has taken off recently with a strong development of experimental and theoretical investigations within the last few years<sup>1</sup>. In particular, much advantage has been taken of various Feshbach resonances which offer the possibility observing experimentally the so called BEC-BCS crossover. This has been done in particular in <sup>6</sup>Li and in <sup>40</sup>K. In the weak coupling limit of small negative scattering length, which is realized far away on one side of the resonance, the corresponding weak attractive interaction between fermions leads to a BCS type condensate of Cooper pairs. On the other side of the resonance, where the scattering length is positive, weakly bound dimers, or molecules, consisting of two different fermions are formed. When one goes far enough of the resonance on this positive side, one obtains a weakly interacting gas of these dimers, which may in particular form a Bose-Einstein condensate, as it has been recently observed experimentally<sup>2,3,4,5</sup>.

In the present paper, motivated by the problem raised by the physics of this dilute gas of composite bosons, we will deal with the dimer-dimer elastic scattering and present an exact diagrammatic approach to its solution. This will be done by staying in the so-called resonance approximation which is quite suited to the physical situation found with a Feshbach resonance. In this case the (positive) scattering length greatly exceeds the characteristic radius  $r_0$  for the attractive interaction between fermionic atoms. A problem of this kind was first investigated by Skorniakov and Ter-Martirosian<sup>6</sup> in the case of the 3-body fermionic problem. They showed that the scattering length of a fermion on a weakly bound dimer is determined by a single parameter, namely the two-body scattering length  $a_F$  between fermions, and it is equal to  $1.18a_F$  in the zero-range limit for the interatomic potential. A similar situation is found in the case of four fermions, where the dimer-dimer scattering length is fully determined by this same scattering length  $a_F$ .

In a study of the crossover problem Haussmann<sup>7</sup> calculated this scattering length of composite bosons  $a_B$  at the level of the Born approximation and found it equal to  $2a_F$ . This result was later on much improved by Pieri and Strinati<sup>8</sup>, who took into account the repeated scattering of these composite bosons in the ladder approximation. This diagrammatic approach led them to a scattering length approximately equal to  $a_B \simeq 0.75a_F$ . However, this ladder approximation is not exact, because it misses an infinite number of other diagrams which in principle lead to a contribution of the same order of magnitude as those taken into account. Very recently this problem has been solved exactly by Petrov, Salomon, and Shlyapnikov<sup>9,10</sup> who found for the scattering length of these composite bosons  $a_B = 0.6a_F$ . This has been achieved by solving directly the Schrödinger equation for four fermions, using the well-known method of pseudopotentials. Here we will give an exact solution of this scattering problem of two weakly bound

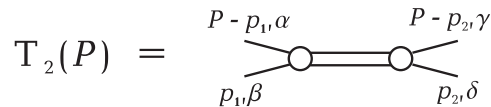


FIG. 1: The graphic representation of the two particles vertex  $T_2(P)$  (the four external propagators do not belong to  $T_2(P)$ ).

dimers, using a diagrammatic approach in the resonance approximation, which can be seen as a bridge between the approach of Pieri and Strinati<sup>8</sup> and the exact result of Petrov, Salomon, and Shlyapnikov<sup>9,10</sup>.

In order to show the strength and the versatility of our approach, we make use of it to obtain new results for various systems, in the two-dimensional (2D) case which is of interest not only for cold gases, but also for high  $T_c$  superconductivity. Specifically we consider first a system of resonantly interacting bosons. We calculate exactly the three bosons  $bbb$  and four bosons  $bbbb$  bound state energies in this case. We also make use of our approach for the study of 2D bosons interacting resonantly with fermions. In this case we calculate exactly the bound state energies of two bosons plus one fermion  $bbf$ , two bosons plus two fermions  $bf_\uparrow bf_\downarrow$ , and three bosons plus one fermion  $bbbf$ . In this respect the present paper is in the line of previous results obtained by some of us. Indeed the possibility of two fermions<sup>11,12</sup>  $ff$  and two bosons<sup>13</sup>  $bb$  pairing was predicted, as well as the creation<sup>14</sup> of a composite fermion  $bf$  in resonantly interacting ( $a \gg r_0$ ) 2D Fermi-Bose mixtures.

## II. THREE PARTICLES SCATTERING

As a preliminary exercise we will rederive the result of Skorniakov and Ter-Martirosian for the dimer-fermion scattering length  $a_3$  using the diagrammatic method<sup>15</sup>. Following Skorniakov and Ter-Martirosian, in the presence of the weakly bound resonance level  $-E_b$  (with  $E_b > 0$ ), we can limit ourselves to the zero-range interaction potential between fermions in the scattering of these two particles. The two-fermion vertex can be approximated by a simple one-pole structure, which reflects the presence of the s-wave resonance level in the spin-singlet state, and is essentially given by the scattering amplitude, namely:

$$T_{2\alpha\beta;\gamma\delta}(P) = T_2(P) \times (\delta_{\alpha,\gamma}\delta_{\beta,\delta} - \delta_{\alpha,\delta}\delta_{\beta,\gamma}) \cdot (\delta_{\alpha,\uparrow}\delta_{\beta,\downarrow} + \delta_{\alpha,\downarrow}\delta_{\beta,\uparrow}) = T_2(P)\chi(\alpha,\beta)\chi(\gamma,\delta), \quad (1)$$

$$T_2(P) = \frac{4\pi}{m^{3/2}} \frac{\sqrt{E_b} + \sqrt{\mathbf{P}^2/4m - E}}{E - \mathbf{P}^2/4m + E_b}, \quad \chi(\alpha,\beta) = \delta_{\alpha,\uparrow}\delta_{\beta,\downarrow} - \delta_{\alpha,\downarrow}\delta_{\beta,\uparrow}, \quad (2)$$

where  $P = \{\mathbf{P}, E\}$ ,  $E$  is the total frequency and  $\mathbf{P}$  is the total momentum of incoming particles,  $m$  is the fermionic mass,  $E_b = 1/ma_F^2$ . Indices  $\alpha, \beta$  and  $\gamma, \delta$  denote the spin states of incoming and outgoing particles. The function  $\chi(\alpha, \beta)$  stands for the spin singlet state. We will draw this vertex in the way, shown on Fig. 1, where the double line can be regarded as a propagating dimer.

The simplest process that contributes to dimer-fermion interaction is the exchange of a fermion. We denote the corresponding vertex as  $\Delta_3$  and it is described by the diagram on Fig. 2. Its analytical expression reads

$$\Delta_{3\alpha,\beta}(p_1, p_2; P) = -\delta_{\alpha,\beta} G(P - p_1 - p_2), \quad (3)$$

where  $G(p) = 1/(\omega - \mathbf{p}^2/2m + i0_+)$  is the bare fermion Green's function. The minus sign in the right hand side of Eq.(3) comes from the permutation of the two fermions. In order to obtain the full dimer-fermion scattering vertex  $T_3$  we need to sum up all possible diagrams with indefinite number of  $\Delta_3$  blocks. In the present case these diagrams have a ladder structure. It is obvious that the spin projection is conserved in every order in  $\Delta_3$  and thus  $T_{3\alpha,\beta} = \delta_{\alpha,\beta} T_3$ . An equation for  $T_3$  will have the diagrammatic representation shown in Fig. 3. It is obtained by writing that either the simplest exchange process occurs alone, or it is followed by any other process. In analytical form it reads

$$T_3(p_1, p_2; P) = -G(P - p_1 - p_2) - \sum_q G(P - p_1 - q)G(q) T_2(P - q) T_3(q, p_2; P), \quad (4)$$

where  $\sum_q \equiv i \int d^3q d\Omega / (2\pi)^4$ . We can integrate out the frequency  $\Omega$  in Eq.(4) by closing the integration contour in the lower half-plane, since both  $T_2(P - q)$  and  $T_3(q, p_2; P)$  are analytical functions of  $\Omega$  in this region (this property for  $T_3(p_1, p_2; P)$  results from Eq.(4) itself). Hence only the "on the shell" value  $T_3(\{\mathbf{q}, q^2/2m\}, p_2; P)$  comes in the right-hand side of Eq.(4). Moreover, if we are interested in the low-energy s-wave dimer-fermion scattering length  $a_3$ , we have to put  $P = \{\mathbf{P}, E\} = \{\mathbf{0}, -E_b\}$  and  $p_2 = 0$ . Hence Eq.(4) reduces to an equation for the "on the shell" value of  $T_3(p_1, p_2; P)$ . Taking into account the standard relation between  $T$ -matrix and scattering amplitude (with



FIG. 2: The graphic representation of the simplest dimer-fermion scattering process  $\Delta_3$  (the two external fermion propagators and the two external dimer propagators do not belong to  $\Delta_3$ ).

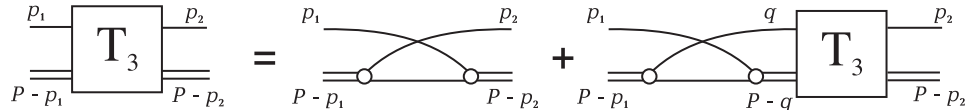


FIG. 3: The diagrammatic representation of the equation for the full dimer-fermion scattering vertex  $T_3$ .

reduced mass) and the fact that, from Eq.(1),  $T_2$  has an additional factor  $8\pi/(m^2 a_F)$  compared to a standard boson propagator, we find that the full vertex  $T_3$  is connected with  $a_3$  by the following relation:

$$\left(\frac{8\pi}{m^2 a_F}\right) T_3(0, 0; \{\mathbf{0}, -E_b\}) = \frac{3\pi}{m} a_3. \quad (5)$$

This leads to introduce a new function  $a_3(\mathbf{k})$  defined by

$$a_3(\mathbf{k}) = \frac{4}{3m} \left( \sqrt{mE_b} + \sqrt{3k^2/4 + mE_b} \right) T_3(\{\mathbf{k}, k^2/2m\}, 0; \{\mathbf{0}, -E_b\}). \quad (6)$$

and substituting it in Eq.(4), we obtain Skorniakov - Ter-Martirosian equation for the scattering amplitude:

$$\frac{(3/4) a_3(\mathbf{k})}{\sqrt{mE_b} + \sqrt{3k^2/4 + mE_b}} = \frac{1}{k^2 + mE_b} - 4\pi \int \frac{d\mathbf{q}}{(2\pi)^3} \frac{a_3(\mathbf{q})}{q^2 (k^2 + q^2 + \mathbf{k}\cdot\mathbf{q} + mE_b)}. \quad (7)$$

Solving this equation one obtains the well known result<sup>6</sup> for the dimer-fermion scattering length  $a_3 = a_3(0) = 1.18a_F$ .

### III. DIMER - DIMER SCATTERING

By now we can proceed to the problem of the dimer-dimer scattering. This problem was previously solved by Petrov et al.<sup>9,10</sup> via studying Schrödinger equation for a 4-fermions wave function. Our diagrammatic approach is conceptually close to Petrov's one. Its basic point is that it requires the introduction of a special vertex which describes an interaction of one dimer as a single object with the two fermions constituting the other dimer.

Let us investigate all the possible types of diagrams that contribute to the dimer-dimer scattering vertex  $T_4$ . In this process both dimers are temporarily "broken" in their fermionic components, which means that the fermions of one dimer exchange and/or interact with the fermions of the other dimer. The simplest process is an exchange of fermions by two dimers shown on Fig. 4a. More complicated diagrams are composed by introducing intermediate interactions between exchanging fermions (see Fig. 4b,c). As long as one of the fermions does not interact or exchange with the other ones, all these complications can be summed up in the  $T_3$  block (see Fig. 4d) which describes, as we have seen in the preceding section, the scattering of a fermion on a dimer. Furthermore we may exchange bachelor fermions participating in the  $T_3$  scattering. The resulting series has the diagrammatic structure shown on Fig. 4e. This series describes a "bare" interaction between dimers. The last obvious step is to compose ladder type diagrams from this "bare" interaction. A typical ladder diagram is shown on Fig. 4f. These general ladder diagrams describe all possible processes which contribute to the dimer-dimer scattering.

The fact that the  $T_4$  vertex should be expressed in terms of  $T_3$  was first noticed by Weinberg in his work on multiparticle scattering problems<sup>16</sup>. Note that a calculation of the diagrams shown on Fig. 4e, f requires information about an off-shell matrix  $T_3$ , that is about a matrix with arbitrary relation between frequencies and momenta of incoming and outgoing particles. On the other hand, for the calculation of the dimer-fermion scattering length  $a_3$  in Eq.(7), only the simpler on-shell structure of  $T_3$  is required as we have seen in the preceding section. Luckily, as we will see now, we can exclude  $T_3$  from our considerations and express  $T_4$  only in terms of  $T_2$ . By doing this we reduce the number of integral equations required for the calculation of the dimer-dimer scattering length  $a_4$ .

Since, as we have just seen, it is impossible to construct a closed equation for the dimer-dimer scattering vertex  $T_4$ , we wish to find an alternative way for taking into account in one equation all the diagrams contributing to

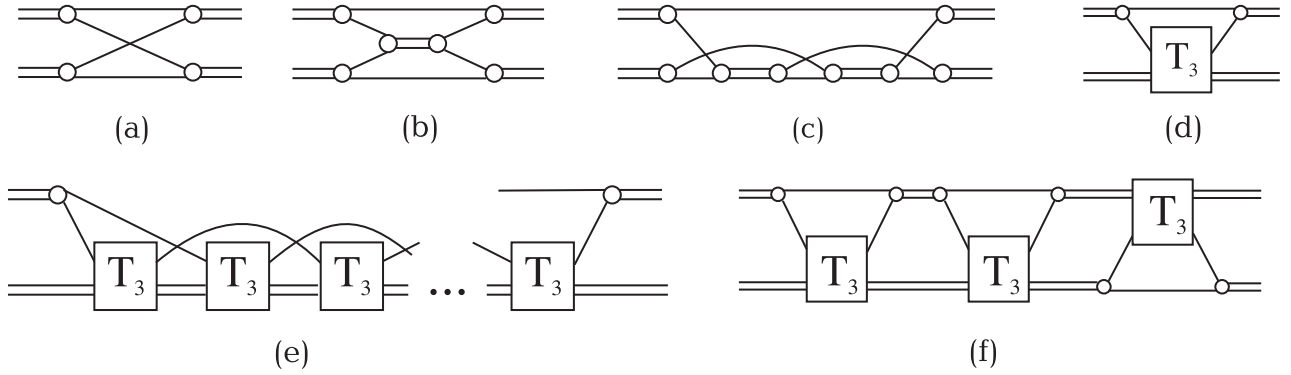


FIG. 4: The graphic representation of the dimer-dimer scattering processes contributing to  $T_4$ .

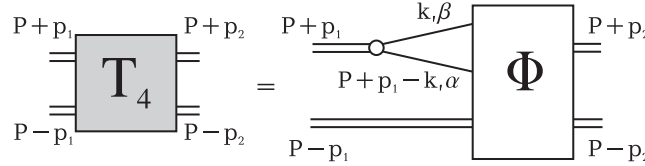


FIG. 5: Diagrammatic representation of the relation between the full dimer-dimer scattering matrix  $T_4$  and the vertex  $\Phi$ .

dimer-dimer scattering. Inspired by the work of Petrov et al.<sup>9,10</sup> and looking at the diagrams we have considered above, we are naturally lead to look for a special vertex that describes the interaction of two fermions, constituting the first dimer, with the second dimer taken as a single object. This vertex would be the sum of all diagrams with two fermions and one dimer as incoming lines. It would be natural to suppose that these diagrams should have the same set of outgoing – two fermionic and one dimer – lines. However in this case there will be a whole set of disconnected diagrams contributing to our sum that describe interaction of a dimer with only one fermion. As it was pointed out by Weinberg<sup>16</sup>, one can construct a good integral equation of Lippmann-Schwinger type only for connected class of diagrams. Thus we are forced to pay our attention to the vertex  $\Phi_{\alpha\beta}(q_1, q_2; p_2, P)$  corresponding to the sum of all diagrams with one incoming dimer, two incoming fermionic lines and two outgoing dimer lines (see Fig. 5). This is also quite natural from our view point since, in our scattering problem we are interested in a final state with two outgoing dimers. Indeed once this vertex  $\Phi_{\alpha\beta}(q_1, q_2; p_2, P)$  is known, it is straightforward to calculate the dimer-dimer scattering vertex  $T_4(p_1, p_2; P)$  which is given by:

$$T_4(p_1, p_2; P) = \frac{1}{2} \sum_{k; \alpha, \beta} \chi(\alpha, \beta) G(P + p_1 - k) G(k) \Phi_{\alpha\beta}(P + p_1 - k, k; p_2, P). \quad (8)$$

The corresponding diagrammatic representation is given in Fig. 5. One can readily verify that, in any order of interaction,  $\Phi$  contains only connected diagrams.

The spin part of the vertex  $\Phi_{\alpha, \beta}$  has the simple form  $\Phi_{\alpha, \beta}(q_1, q_2; P, p_2) = \chi(\alpha, \beta) \Phi(q_1, q_2; P, p_2)$ . The diagrammatic representation of the equation for  $\Phi$  is given in Fig. 6. One can assign some "physical meaning" to the processes described by these diagrams. The diagram of Fig. 6a represents the simplest exchange process in a dimer-dimer interaction. The diagram of Fig. 6b accounts for a more complicated nature of a "bare" dimer-dimer interaction. Finally the diagram of Fig. 6c allows for a multiple dimer-dimer scattering via a "bare" interaction (it generates ladder-type diagrams analogous to those of Fig. 4f). The last term in Fig. 6 means that we should add another set of three diagrams analogous to those of Fig. 6a, b, c but with the two incoming fermions ( $q_1$  and  $q_2$ ) exchanged. The diagrammatic representation translates into the following analytical equation for the vertex  $\Phi$ :

$$\begin{aligned} \Phi(q_1, q_2; p_2, P) = & -G(P - q_1 + p_2)G(P - q_2 - p_2) - \sum_k G(k)G(2P - q_1 - q_2 - k)T_2(2P - q_1 - k)\Phi(q_1, k; p_2, P) \\ & - \frac{1}{2} \sum_{Q, k} G(Q - q_1)G(2P - Q - q_2)T_2(2P - Q)T_2(Q)G(k)G(Q - k)\Phi(k, Q - k; p_2, P) + (q_1 \leftrightarrow q_2). \quad (9) \end{aligned}$$

Finally let us also indicate that it is possible to rederive the same set of equations, purely algebraically, by taking a complementary point of view. Instead of focusing, as we have done, on the free fermions lines as soon as a dimer

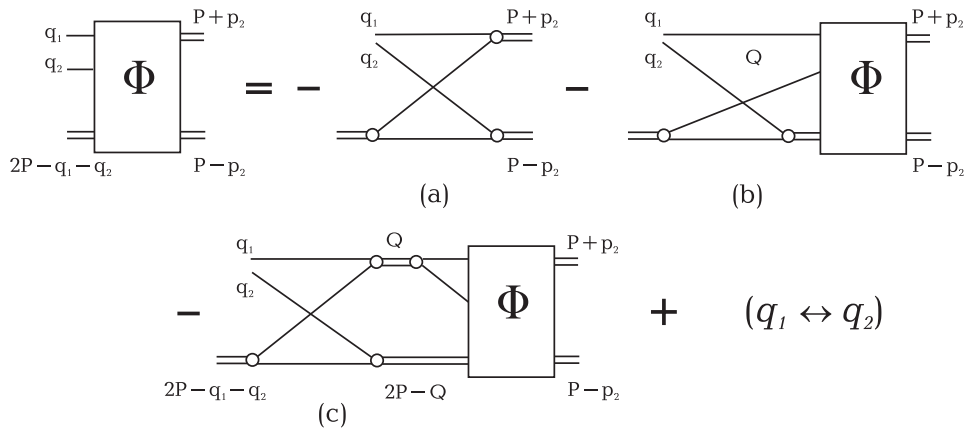


FIG. 6: The diagrammatic representation of the integral equation for the function  $\Phi$  introduced by dimer-dimer scattering .

is "broken", we can rather keep track of the fermions which make up a dimer. This leads again automatically to introduce the vertex  $\Phi(q_1, q_2; p_2, P)$ . Then Eq.(9) is recovered when one keeps in mind that, after breaking dimers, one may have propagation of a single dimer and two free fermions before another break (this corresponds to the second term in the right hand side of Eq.(9)). Alternatively one may also have the propagation of two dimers, which leads to the third term in Eq.(9).

Coming back now more specifically to our problem, we can put  $p_2 = 0$  and  $P = \{\mathbf{0}, -E_b\}$  since we are looking for an s-wave scattering length. At this point we have a single closed equation for the vertex  $\Phi$  in momentum representation, which we believe is analogous to Petrov *et al* equation in coordinate representation. To make this analogy more prominent we have to exclude frequencies from the equation by integrating them out. However this exclusion requires some more technical mathematics and we leave it out for Appendix A.

The dimer-dimer scattering length is directly related to the full symmetrized vertex  $T_4(p_1, p_2; P)$ . Just as in the preceding section, taking also statistics into account, we have:

$$\left(\frac{8\pi}{m^2 a_F}\right)^2 T_4(0, 0; \{\mathbf{0} - E_b\}, 0) = \frac{2\pi(2a_B)}{m}. \quad (10)$$

If one skips the second term in Eq. (9), i.e. one omits diagram Fig.6b, one will arrive at the ladder approximation of Pieri and Strinati<sup>8</sup>. The exact equation (9) corresponds to the summation of all diagrams. We have calculated the scattering length in the ladder approximation and the scattering length derived from the exact equation and obtained  $0.78a_F$  and  $0.60a_F$  respectively. Some details on our actual procedure are given in the next section. Thus our results in the ladder approximation are in agreement with the results<sup>8</sup> of Pieri and Strinati and, in the general form, with the results of Petrov *et. al*<sup>9,10</sup>. Note also that our approach allows one to find the dimer-dimer scattering length in the 2D case (this problem was previously solved by Petrov *et. al*<sup>17</sup>).

Finally we would like to mention that our results allow one to find a fermionic Green's function, chemical potential and sound velocity as a function of  $a_F$  in the case of dilute superfluid bose gas of dimers at low temperatures. The problem of dilute superfluid bose gas of di-fermionic molecules was solved by Popov<sup>18</sup>, and later deeply investigated by Keldysh and Kozlov<sup>19</sup>. Those authors managed to reduce the gas problem to a dimer-dimer scattering problem in vacuum, but were unable to express the dimer-dimer scattering amplitude in a single two-fermion parameter. A direct combination of our results with those ones of Popov, Keldysh and Kozlov allows one to get all the thermodynamical values of a dilute superfluid resonance gas of composite bosons. Another interesting subject for the application of our results will be a high-temperature expansion for the thermodynamical potential and sound velocity in the temperature region  $T \sim T_* \sim E_b$ , where the composite bosons begin to appear.

#### IV. PRACTICAL IMPLEMENTATION

Let us give now some details on the way in which we have solved effectively the above equations. Actually we have dealt with two problems, the scattering length calculation discussed above and the bound states problem to be discussed below. Our two problems are quite closely related since, for the scattering length problem, we look for the scattering amplitude at zero outgoing wavevectors and energy for two dimers, while for the bound states we look for divergences of this same scattering amplitude at negative energy. As already indicated, in both cases the situation is

somewhat simplified with respect to the variables we have to consider, due to the specific problem we handle. First with respect to  $P = \{\mathbf{P}, E\}$ , we have  $\mathbf{P} = \mathbf{0}$  since we work naturally in the rest frame of the four particles. Moreover, with respect to the total energy,  $E = -\epsilon E_b$  is negative. Specifically  $\epsilon = 1$  when we look for the scattering length. Or when we consider bound states  $\epsilon$  gives the energy of the bound states we are looking for. Next, with respect to parameter  $p_2 \equiv \{\mathbf{p}_2, \bar{p}_2\}$  which characterizes the outgoing dimers, we will have naturally  $\mathbf{p}_2 = \mathbf{0}$  as we have said since we consider zero outgoing wavevectors. Since we will evaluate  $\bar{p}_2$  on the shell, we have merely  $\bar{p}_2 = 0$ , and this parameter drops out. Hence in the following we do not write anymore explicitly the value of parameter  $P$ . Both for the scattering length problem and the bound states problem, we have followed two main routes.

In our first route, we have written a specific integral equation for  $T_4(p_1, p_2)$ , which is then solved numerically. The details of our derivation for this integral equation are given in Appendix B. The kernel for this equation is itself obtained from a vertex  $\Gamma$ . The defining integral equation Eq.(B2) for this vertex has been inverted numerically, by calculating the inverse matrix, to obtain the vertex  $\Gamma(q_1, q_2; p_2)$ . We have used<sup>20</sup> LU factorization and Gauss quadrature. The result has then been substituted in Eq.(B1) which gives the kernel  $\Delta_4(p_1, p_2)$  coming in the integral equation Eq.(B3). The solution of this last equation is naturally also handled numerically, for example by finding the eigenvalues of the kernel for the bound states problem.

In our second route we have kept both functions  $T_4$  and  $\Phi$ . In the following we do not write anymore the parameter  $p_2$  which takes always the trivial value  $p_2 = 0$ , as explained above. Hence we are left with  $T_4(p_1)$  which, because of rotational invariance, depends only on the energy  $\bar{p}_1$  and the modulus  $|\mathbf{p}_1|$  of the momentum. For brevity we denote this quantity  $t_4(|\mathbf{p}_1|, \bar{p}_1)$ . On the other hand it is shown in Appendix A that, in order to evaluate the second term in the right-hand side of Eq.(9), we need only the evaluation of  $\Phi(q_1, q_2)$  on the shell, which we denote as  $\phi(\mathbf{q}_1, \mathbf{q}_2)$ . It depends only on the three variables  $|\mathbf{q}_1|$ ,  $|\mathbf{q}_2|$  and the angle between these two vectors. Hence it is enough to write Eq.(9) only for  $q_1$  and  $q_2$  taking on the shell values. From Eq.(9) this leads for  $\phi(\mathbf{q}_1, \mathbf{q}_2)$  to the following more convenient equation:

$$\phi(\mathbf{q}_1, \mathbf{q}_2) = -\frac{1}{(|E| + \mathbf{q}_1^2/m)(|E| + \mathbf{q}_2^2/m)} + \int \frac{d^D \mathbf{k}}{(2\pi)^D} \frac{2m t_2(2|E| + [2\mathbf{k}^2 + 2\mathbf{q}_1^2 + (\mathbf{k} + \mathbf{q}_1)^2]/4m) \phi(\mathbf{q}_1, \mathbf{k})}{4m|E| + \mathbf{k}^2 + \mathbf{q}_1^2 + \mathbf{q}_2^2 + (\mathbf{k} + \mathbf{q}_1 + \mathbf{q}_2)^2} \quad (11)$$

$$- \frac{1}{2} \sum_Q \frac{(2m)^2 t_2(|E| + \bar{Q} + \mathbf{Q}^2/4m) t_2(|E| - \bar{Q} + \mathbf{Q}^2/4m) t_4(|\mathbf{Q}|, \bar{Q})}{(2m(|E| - \bar{Q}) + \mathbf{q}_1^2 + (\mathbf{Q} + \mathbf{q}_1)^2)(2m(|E| + \bar{Q}) + \mathbf{q}_2^2 + (\mathbf{Q} + \mathbf{q}_2)^2)} + (\mathbf{q}_1 \leftrightarrow \mathbf{q}_2)$$

where the dimer propagator  $t_2(x)$  depends on the space dimension  $D$ . For  $D = 3$  it is given from Eq.(1) by  $t_2(x) \equiv -4\pi/[m^{3/2}(\sqrt{x} - \sqrt{E_b})]$ , while for  $D = 2$  according to Eq.(21) we have  $t_2(x) \equiv -4\pi/[m \ln(x/E_b)]$ . In the third term the angular integration can be performed analytically, and one is left with double integrals for the last two terms, for the  $3D$  as well as for the  $2D$  case. It is actually quite convenient, in the last term, to deform the  $\bar{Q}$  contour from  $]-\infty, \infty[$  to  $]-i\infty, i\infty[$  by rotating it by  $\pi/2$ . No singularity is met in this deformation, and one is left to deal only with real quantities.

The above equation has to be supplemented by a corresponding equation for  $t_4(|\mathbf{q}|, \bar{q})$  obtained from the definition Eq.(8). The important point is that the additional integrations can be performed analytically, owing to the various invariances under rotations found in the resulting terms. We just give here as an intermediate step the structure of the resulting equation:

$$t_4(k, iz) = S(k, z) + \int_0^\infty dp_1 \int_0^\infty dp_2 \int_0^{2\pi} d\alpha I(k, z, p_1, p_2, \alpha) t_2(2|E| + [3\mathbf{p}_1^2 + 3\mathbf{p}_2^2 + 2\mathbf{p}_1 \cdot \mathbf{p}_2]/4m) \phi(\mathbf{p}_1, \mathbf{p}_2) \quad (12)$$

$$+ \int_0^\infty dK \int_0^\infty dZ J(k, z, K, Z) |t_2(|E| + iZ + K^2/4m)|^2 t_4(K, iZ)$$

where  $\alpha$  is the angle between  $\mathbf{p}_1$  and  $\mathbf{p}_2$ . Here  $S(k, z)$ ,  $I(k, z, p_1, p_2, \alpha)$  and  $J(k, z, K, Z)$  are analytically known functions of the variables (except that  $J$  requires to perform numerically a simple integration to be obtained, see below). In this equation and in particular in its last term, we have already gone to the purely imaginary frequency variable for  $t_4$ . The resulting  $t_4(x, iz)$  turns out to be real and even with respect to  $z$ .

To be fully specific let us now give the actual self-contained integral equations which we have solved. We restrict ourselves to the  $3D$  case and to the *bfbf* case (implying  $\alpha = 1$ ), corresponding to the dimer scattering problem treated<sup>9,10</sup> by Petrov *et al.* The only generalization is that we keep  $E = -\epsilon|E_b|$ , instead of setting  $\epsilon = 1$  as we should if we considered only the scattering length problem. For clarity we write the resulting equations with dimensionless quantities, where  $1/a$  has been taken as unit wavevector, and  $|E_b| = 1/ma^2$  as energy unit. For simplicity we keep basically the same notations for the various variables. We just indicate by a bar over the function name that they are expressed in reduced units, with reduced variables (actually we write  $\bar{t}_4(k, z)$  instead of  $t_4(k, iz)$ , and there is a change of sign between  $\phi(\mathbf{q}_1, \mathbf{q}_2)$  and  $\bar{\phi}(\mathbf{p}_1, \mathbf{p}_2)$ ). Equations for other cases and dimensions are completely similar

with only few changes in coefficients, signs (for the particle statistics), for the expression of  $\bar{t}_2(x)$  and for the explicit functions coming from analytical angular integrations.

We obtain:

$$\begin{aligned} \bar{\phi}(\mathbf{p}_1, \mathbf{p}_2) = & \frac{1}{(\epsilon + p_1^2)(\epsilon + p_2^2)} + \frac{1}{\pi} \int_0^\infty k^2 dk \int_0^\pi \sin \theta d\theta \frac{\bar{\phi}(\mathbf{p}_1, \mathbf{k}) \bar{t}_2(2\epsilon + (3p_1^2 + 3k^2 + 2kp_1 \cos \theta)/4)}{\sqrt{A_+ A_-}} + (\mathbf{p}_1 \leftrightarrow \mathbf{p}_2) \\ & + \frac{8}{\pi p_1 p_2} \int_0^\infty dz \int_0^\infty dk \bar{t}_4(k, z) |\bar{t}_2(\epsilon + k^2/4 + iz)|^2 I(B_1, B_2, \alpha) \end{aligned} \quad (13)$$

with  $A_\pm = 2\epsilon + p_1^2 + p_2^2 + k^2 + p_1 p_2 \cos \alpha + k p_1 \cos \theta + k p_2 \cos(\alpha \pm \theta)$ , and  $\alpha$  is the angle between  $\mathbf{p}_1$  and  $\mathbf{p}_2$ , while  $\theta$  is the polar angle of  $\mathbf{k}$  with  $\mathbf{p}_1$ . We have simply set now  $\bar{t}_2(x) = [1 - \sqrt{x}]^{-1}$ . Here we have also defined the function:

$$I(B_1, B_2, \alpha) = \Re \epsilon \frac{1}{2\sqrt{E}} \ln \frac{B_1 B_2^* + \cos \alpha + \sqrt{E}}{B_1 B_2^* + \cos \alpha - \sqrt{E}} \quad (14)$$

$$E = B_1^2 + B_2^{*2} + 2B_1 B_2^* \cos \alpha - \sin^2 \alpha \quad (15)$$

$$B(p, k, z) = \frac{1}{kp} [\epsilon + p^2 + \frac{k^2}{2} - iz] \quad (16)$$

$$B_i \equiv B(p_i, k, z) \quad (17)$$

The corresponding equation for  $\bar{t}_4(k, z)$  is:

$$\begin{aligned} \bar{t}_4(k, z) = & -\frac{1}{4\pi k z} \ln \frac{1 + \cos \gamma + 2\sqrt{\cos \gamma} \cos(\varphi - \gamma/2)}{1 + \cos \gamma + 2\sqrt{\cos \gamma} \cos(\varphi + \gamma/2)} \\ & - \frac{1}{\pi^3 k^2} \int_0^\infty p_1 dp_1 \int_0^\infty p_2 dp_2 \int_0^\pi \sin \alpha d\alpha \bar{\phi}(\mathbf{p}_1, \mathbf{p}_2) \bar{t}_2(2\epsilon + (3p_1^2 + 3p_2^2 + 2p_1 p_2 \cos \alpha)/4) I(B_1, B_2, \alpha) \\ & - \frac{1}{2\pi^3 k} \int_0^\infty K dK \int_0^\infty dZ \bar{t}_4(K, Z) |\bar{t}_2(\epsilon + K^2/4 + iZ)|^2 \bar{J}(k, z, K, Z) \end{aligned} \quad (18)$$

with  $\varphi = \arctan(k/2)$  and  $\gamma = \arctan[4z/(4 + k^2)]$  and we have defined the function:

$$\bar{J}(k, z, K, Z) = \int_0^\infty dx \frac{1}{\epsilon + x^2 + \frac{k^2 + K^2}{4}} \ln \frac{C(x, k, K, Z)}{C(x, -k, K, Z)} \ln \frac{C(x, K, k, z)}{C(x, -K, k, z)} \quad (19)$$

$$C(x, k, K, Z) = [\epsilon + (x + \frac{k}{2})^2 + \frac{K^2}{4}]^2 + Z^2 \quad (20)$$

It is seen on these integral equations for our two unknown functions  $\bar{t}_4(x, z)$  and  $\bar{\phi}(\mathbf{p}_1, \mathbf{p}_2)$  that they require only at most a triple integrals to be performed numerically. In this sense they are not numerically more complicated than the work involved in solving directly for the corresponding Schrödinger equation, as it has been done<sup>9,10</sup> by Petrov *et al.* Indeed these integrals require only a few appropriate change of variables to take care of singular behaviours occuring on some boundaries. Otherwise they have been performed with unsophisticated integration routine.

In the case of the scattering length a mere iteration algorithm has been found to lead rapidly to the solution (provided an appropriate exact algebraic manipulation is made to make the iteration convergent). In this way we have been able to handle  $45 \times 45 \times 45$  matrices (for the three variables entering  $\bar{\phi}(\mathbf{p}_1, \mathbf{p}_2)$ ). This size is large enough to allow improved precision by extrapolation to infinite size, although we have not done it in the present case, but rather for the ground state of the *bbbb* complex discussed below. This leads to the result  $a_B = 0.60 a_F$  in full agreement with Petrov<sup>9,10</sup> *et al.*, within a quite reasonable computing time on (nowadays) unsophisticated computer. We have not tried to improve on the accuracy of the result, since there is no basic interest. In the case of the bound states, to be described below, we have proceeded to a straight diagonalization of the matrix equivalent to the right hand sides of Eq.(13) and Eq.(18) with the Lapack library algorithm. In the 2D case, it is worth noticing that, because of the logarithmic dependence of  $\bar{t}_2(x)$  on  $x$ , it is quite an improvement to make the change of variables  $K = \epsilon^{1/2} K'$  and  $Z = \epsilon Z'$ , and so on, since the more appropriate variable turns out to be  $\ln \epsilon$  rather than  $\epsilon$  itself.

## V. NEW RESULTS IN A 2D CASE

We will now apply the diagrammatic approach developed in the previous sections (see also Appendix A) to get new results for the systems of resonantly interacting particles in a 2D case.

As it was first shown by Danilov<sup>21</sup> (see also a paper by Minlos and Fadeev<sup>22</sup>) in the 3D case, the problem of three resonantly interacting bosons could not be solved in the resonance approximation. This statement stems from the fact that in the case of identical bosons the homogeneous part of Skorniakov-Ter-Martirosian equation (7) has a non-zero solution at any energies. The physical meaning of this mathematical feature was elucidated by Efimov, who showed that a two-particle interaction leads to the appearance of an attractive  $1/r^2$  interaction in a three-body system. Since in the attractive  $1/r^2$  potential a particle can fall into the center, the short range physics is important and one can not replace the exact pair interaction by its resonance approximation.

On the contrary in the case of the 2D problem the phenomena of the particle fall into the center is absent and one can utilize the resonant approximation<sup>23,24</sup>. Therefore it is possible to describe three- and four-particle processes in terms of the two-particle binding energy  $E_b = 1/ma^2$  only (below, for simplicity we will assume that all particles under consideration have the same mass  $m$ ). We will leave aside the problem of composite particles scattering and will concentrate on the problem of binding energies of complexes of three and four particles.

As well as in the case of the 3D problem, the cornerstone in the diagrammatic technique is the two-particle resonance scattering vertex  $T_2$  (see Fig.1). For two resonantly interacting particles with total mass  $2m$  it reads in 2D:

$$T_2(P) = -\frac{4\pi}{m} \frac{\alpha}{\ln(\{\mathbf{P}^2/4m - E\}/|E_B|)}, \quad (21)$$

where we introduce a factor  $\alpha = \{1, 2\}$  in order to take into account whether two particles are indistinguishable or not. That is  $\alpha = 2$  for the case of a resonance interaction between identical bosons, while  $\alpha = 1$  for the case of a resonance interaction between fermion and boson, or for the case of two distinguishable fermions.

### A. Three particles in 2D

We start with a system of three resonantly interacting identical bosons -  $bbb$  - in 2D. An equation for the dimer-boson scattering vertex  $T_3$  which describes interaction of three bosons has the same diagrammatic form as the one shown on the Fig.3, however there are small changes in the rules for its analytical evaluation. The resulting equation reads:

$$T_3(p_1, p_2; P) = G(P - p_1 - p_2) + \sum_q G(P - p_1 - q)G(q) T_2(P - q) T_3(q, p_2; P), \quad (22)$$

where we have now  $\sum_q \equiv i \int d^2q d\Omega / (2\pi)^3$ ,  $P = \{\mathbf{0}, E\}$ , and one should put  $\alpha = 2$  for the two-particle vertex  $T_2$  in Eq.(21). The opposite signs in Eq. (4) for fermions and Eq. (22) for bosons are due to the permutational properties of the involved particles : an exchange of fermions (see Fig.2) results in a minus sign, while an analogous exchange of bosons brings no extra minus. Finally, as we mentioned above, we note that three-particle s-wave (s-wave channel of a boson-dimer scattering) binding energies  $E_3$  correspond to the poles of  $T_3(0, 0; \{\mathbf{0}, -|E_3|\})$  and, consequently, at energies  $E = E_3$  the homogeneous part of Eq. (22) has a non-zero solution. Solving Eq. (22) we find that a complex of three identical bosons has two s-wave bound states  $E_3 = -16.5 E_b$  and  $E_3 = -1.27 E_b$  in accordance with the previous results of Bruch and Tjon<sup>23,24</sup>.

Let us now consider a complex -  $fbf$  - consisting of one fermion and two bosons. As noted above we take bosons and fermions with equal masses  $m_b = m_f = m$ . We assume that a fermion-boson interaction  $U_{fb}$ , characterized by the length  $r_{fb}$ , yields a resonant two-body bound state with an energy  $E = -E_b$ . In the same time a boson-boson interaction  $U_{bb}$ , characterized by the interaction length  $r_{bb}$ , does not yield a resonance. Hence if we are interested in the low-energy physics the only relevant interaction is  $U_{fb}$  and we can ignore the boson-boson interaction  $U_{bb}$ , the latter would give small corrections of the order  $|E_B|mr_{bb}^2 \ll 1$  at low energies. In order to determine three-particle bound states one has to find poles in the dimer-boson scattering vertex  $T_3$ . Since we neglect the boson-boson interaction  $U_{bb}$  the vertex  $T_3$  is described by the same diagrammatic equation of Fig. 3 as for the problems of three bosons. The analytical form of this equation also coincides with Eq. (22) with the minor difference that the resonance scattering vertex  $T_2$  now corresponds to the interaction between a boson and a fermion, and therefore we should put  $\alpha = 1$  in Eq. (21) for  $T_2$ . Solving the equation for  $T_3$  we find that  $fbf$  complex has only one s-wave bound state with the energy  $E_3 = -2.39 E_b$ . Note that a complex -  $bff$  - consisting of a boson and two spinless identical fermions with resonance interaction  $U_{fb}$  does not have any three-particle bound states.

### B. Four particles in 2D

After solving the above three-particle problems we may proceed to the complexes consisting of four particles. At first we will consider four identical resonantly interacting bosons  $bbbb$ <sup>25</sup>. Any two bosons would form a stable dimer



with binding energy  $E = -E_b$ . We are going to find a four-particle binding energy as an energy of an s-wave bound state of two dimers. Generally speaking a bound state could emerge in channels with larger orbital moments, however this question will be a subject of further investigations. Just as in the preceding subsection, in order to find a binding energy we should examine the analytical structure of the dimer-dimer scattering vertex  $T_4$  and find its poles. The set of equations for  $T_4$  has the same diagrammatic structure as those shown on Fig. 5 and Fig. 6. The analytical expression for the first equation reads:

$$T_4(p_1, p_2; P) = \frac{1}{\alpha} \sum_k G(P + p_1 - k)G(k)\Phi(P + p_1 - k, k; p_2, P), \quad (23)$$

and the equation for the vertex  $\Phi$  is:

$$\begin{aligned} \Phi(q_1, q_2; p_2, P) &= G(P - q_1 + p_2)G(P - q_2 - p_2) + \sum_k G(k)G(2P - q_1 - q_2 - k)T_2(2P - q_1 - k)\Phi(q_1, k; p_2, P) \\ &+ \frac{1}{2\alpha} \sum_{Q, k} G(Q - q_1)G(2P - Q - q_2)T_2(2P - Q)T_2(Q)G(k)G(Q - k)\Phi(k, Q - k; p_2, P) + (q_1 \leftrightarrow q_2). \end{aligned} \quad (24)$$

where  $T_2$  should be taken from Eq.(21) and one should put  $\alpha = 2$  for the case of identical resonantly interacting bosons. When we look for the poles of  $T_4$  as a function of the variable  $E$ , with  $P = \{\mathbf{0}, E\}$ , we have naturally to consider only the homogeneous part of this equation. We have found 2 bound states for the  $bbbb$  complex. The values of the total binding energy  $|E_4| = 2|E|$  are given in Table 1 below. Certainly for the validity of our approximation we should have  $|E_4| \ll 1/mr_0^2$ . For the case of four bosons  $bbbb$  it means that  $197 E_b \ll 1/mr_0^2$  and hence  $a/r_0 \gg \sqrt{197}$ . This case can still be considered as quite realistic for the Feshbach resonance situation.

The case of a four-particle complex -  $bf_\uparrow bf_\downarrow$  - consisting of resonantly interacting bosons and fermions is still described by the same equations (23,24) but with parameter  $\alpha = 1$ . In this case we found 2 bound states and they are also listed in Table 1.

In order to obtain bound states of the  $fbbb$  complex one has to find energies  $P = \{\mathbf{0}, E\}$  corresponding to nontrivial solutions of the following homogeneous equation

$$\Phi(q_1, q_2; p_2, P) = \sum_k G(k)G(2P - q_1 - q_2 - k) T_2(2P - q_1 - k) \Phi(q_1, k; p_2, P) + (q_1 \leftrightarrow q_2). \quad (25)$$

This equation corresponds to the diagram of Fig. 6b. We have found a single bound state for this  $fbbb$  complex. Finally we summarize the results concerning binding energies of three and four resonantly interacting particles in 2D in Table 1.

**Table 1. Bound states of resonantly interacting particles in 2D**

| System                      | Relative <sup>1)</sup> interaction | Number of bound states | Energy (in $ E_B $ ) <sup>2)</sup> | $\alpha$ <sup>3)</sup> |
|-----------------------------|------------------------------------|------------------------|------------------------------------|------------------------|
| $bbb$                       | $U_{bb}$                           | 2                      | 1.27 , 16.5                        | 2                      |
| $fbb$                       | $U_{fb}$                           | 1                      | 2.39                               | 1                      |
| $fbbb$                      | $U_{fb}$                           | 1                      | 4.1                                | 1                      |
| $bf_\uparrow bf_\downarrow$ | $U_{fb}$                           | 2                      | 2.8, 10.6                          | 1                      |
| $bbbb$                      | $U_{bb}$                           | 2                      | 22. , 197.                         | 2                      |

<sup>1)</sup>Interaction that yields resonance scattering. All other interactions are negligible.

<sup>2)</sup> $m = m_b = m_f$ .

<sup>3)</sup>The indistinguishability parameter in Eq. (21).

For the  $bbbb$  complex we find the beginning of a continuum of states at  $|E_4|/E_b = 16.5$ , as it should be since this is, within our numerical precision, the binding energy of  $bbb$ . Similarly we find the beginning of a continuum at  $|E_4|/E_b = 2.4$  for the  $fbbb$  and the  $bf_\uparrow bf_\downarrow$  complex, in agreement with the binding energy of  $fbb$ . We display our corresponding results in Fig. 7 and Fig. 8. In all our calculations we find numerically, as a function of  $|E_4|$ , the eigenvalues  $\lambda$  corresponding to the matrix on the right-hand side of our equations, for example Eq. (25). When one of these eigenvalues is equal to 1, this means that the corresponding  $E_4$  is the energy of an eigenstate of our complex. In Fig. 7, we display the first highest eigenvalues for  $|E_4| = 2.4$ , both for the  $bf_\uparrow bf_\downarrow$  case and the  $bbbf$  case. One sees clearly that a fair number of eigenvalues are essentially equal to 1. One could tune them exactly to 1 by changing very

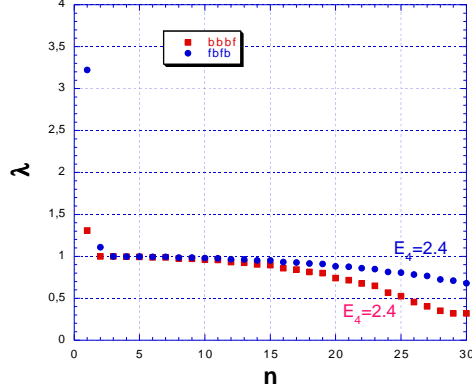


FIG. 7: Eigenvalues  $\lambda$  found for  $|E_4| = 2.4$ , both for the  $bbbf$  case and the  $bf_{\uparrow}bf_{\downarrow}$  case. When one of the eigenvalues is equal to 1,  $E_4$  is the energy of a possible eigenstate of the complex. The number  $n$  appearing on the  $x$  axis is just here to number the first few eigenvalues which are displayed by decreasing order.

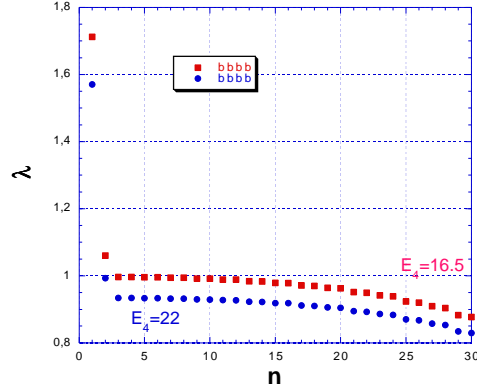


FIG. 8: Eigenvalues  $\lambda$  found for  $|E_4| = 16.5$  and  $|E_4| = 22.$ , for the  $bbbb$  case. When one of the eigenvalues is equal to 1,  $E_4$  is the energy of a possible eigenstate of the complex. The number  $n$  appearing on the  $x$  axis is just here to number the first few eigenvalues which are displayed by decreasing order.

slightly  $|E_4|$ . Hence this corresponds to the beginning of the continuum. By contrast one sees also clearly two isolated eigenvalues larger than 1, for the  $bf_{\uparrow}bf_{\downarrow}$  case, and one eigenvalue larger than 1 for the  $bbbf$  case. One can bring them to  $\lambda = 1$  by increasing  $|E_4|$ , and therefore they correspond to the bound states that we have found. Similarly we display in Fig. 8 the eigenvalues for the  $bbbb$  case, for the value  $|E_4| = 16.5$  corresponding essentially to the threshold for the continuum. Here again one sees many eigenvalues quite close to 1. On the same figure we also show the results of the same calculations for  $|E_4| = 22$ . in order to display the way in which this whole spectrum evolves with  $|E_4|$ . In particular one sees clearly the two isolated eigenvalues, corresponding to the two bound states found in this case. In particular since one of them is equal to 1, this means that the binding energy of one of the bound states is equal to  $22 E_b$ , within our numerical precision.

Note finally that all our calculations correspond to the case of particles with equal masses  $m_f = m_b = m$ , although they can be quite easily generalized to the case of different masses.

## VI. CONCLUSIONS AND DISCUSSION

For the problem of resonantly interacting fermions in 3D we have developed an exact diagrammatic approach that allows to find the dimer-dimer scattering length  $a_B = 0.60a_F$  in exact agreement with known results. This exact diagrammatic solution of the dimer-dimer scattering length problem in 3D opens new horizons for the extension of the self-consistent mean-field schemes of Leggett and Nozières-Schmitt-Rink to the inclusion of the quite essential three and four-particle physics in the two-particle variational wave-functions of the BCS-type. This in turn will help us to get diagrammatically exact results for  $T_c$ , pseudogap and sound velocity in the dilute BEC-limit and to develop a more sophisticated interpolation scheme for these quantities toward the unitarity limit. The work on this very exciting project is now in progress.

We have applied the developed approach to get new results in the 2D case. Namely, we have calculated exactly the binding energies of the following complexes: three bosons  $bbb$ , two bosons plus one fermion  $bbf$ , three bosons plus one fermion  $bbbf$ , two bosons plus two fermions  $bf_\uparrow bf_\downarrow$ , and four bosons  $bbbb$ .

Our investigations enrich the phase-diagram for ultracold Fermi-Bose gases with resonant interaction. They serve as an important step for future calculations of the thermodynamical properties and the spectrum of collective excitations in different temperature and density regimes, in particular in the superfluid domain. Note that in purely bosonic models in 2D or in the Fermi-Bose mixtures in the case of prevailing density of bosons  $n_B > n_F$  a creation of larger complexes consisting of 5, 6 and so on particles is also possible. In fact here we are dealing with the macroscopic phase separation (with the creation of large droplets). The radius of this droplet  $R_N$  for  $N$  bosons in 2D is estimated in<sup>26</sup> on the basis of a variational approach. Note that already for  $N = 5$  the exact calculation of the bound state requires huge computational capability, but it would be interesting to see precisely how this would appear with our approach.

### APPENDIX A: DIMER-DIMER SCATTERING EQUATION. FREQUENCY INTEGRATION

In this Appendix we will show how one can integrate explicitly over the frequency dependence in the dimer-dimer scattering equation (9) (we consider only this case, the other ones considered in Section IV would require trivial modifications). To simplify further computations we slightly change the notation and introduce a chemical potential  $\mu = -E_b/2$  and the single fermion energy  $\xi_{\mathbf{p}} = \mathbf{p}^2/2m - \mu = \mathbf{p}^2/2m + E_b/2$ , with the modified fermion Green's function  $\mathcal{G}(p) = 1/(\omega - \xi_{\mathbf{p}})$ . In the expression Eq.(1) for  $\mathcal{T}_2(Q)$  we have similarly to replace  $E$  by  $E - E_b$ .

The integral equation (9) reads more explicitly (with  $k = \{\mathbf{k}, \omega\}$  and  $Q = \{\mathbf{Q}, \Omega\}$ ):

$$\begin{aligned} \Phi(q_1, q_2) = & -\mathcal{G}(-q_1)\mathcal{G}(-q_2) - i \int_{-\infty}^{\infty} \frac{d\omega}{2\pi} \int \frac{d^3\mathbf{k}}{(2\pi)^3} \mathcal{G}(k)\mathcal{G}(-q_1 - q_2 - k)\mathcal{T}_2(-q_1 - k)\Phi(q_1, k) + \\ & + \frac{1}{2} \int \frac{d^4Q}{(2\pi)^4} \frac{d^4k}{(2\pi)^4} \mathcal{G}(Q - q_1)\mathcal{G}(-Q - q_2)\mathcal{T}_2(-Q)\mathcal{T}_2(Q)\mathcal{G}(k)\mathcal{G}(Q - k)\Phi(k, Q - k) + (q_1 \leftrightarrow q_2). \end{aligned} \quad (\text{A1})$$

From this equation  $\Phi(q_1, q_2) = \Phi(q_2, q_1)$ , as it is obvious physically. Note also that the third term is already explicitly symmetrical in  $q_1 \leftrightarrow q_2$ .

First we note that, from Eq.(A1) itself,  $\Phi(q_1, q_2)$  is analytical with respect to the frequency variables  $\omega_1$  and  $\omega_2$  of the four-vectors  $q_1$  and  $q_2$  in the lower half-planes  $\Im\omega_1 < 0$  and  $\Im\omega_2 < 0$ . This can be seen by assuming this property self-consistently in the right-hand side, and checking that the three terms are then indeed analytical, or equivalently one can proceed to a perturbative expansion. Then, if we make the "on the shell" calculation of  $\Phi(q_1, q_2)$  from Eq.(A1), that is for  $\omega_1 = \xi_{\mathbf{q}_1}$  and  $\omega_2 = \xi_{\mathbf{q}_2}$ , we see that, for second term in the right-hand side, the only singularity in the lower complex plane  $\Im\omega < 0$  is the pole of  $\mathcal{G}(k)$  at  $\omega = \xi_{\mathbf{k}}$ . Hence the integration contour can be closed in the lower half-plane, leading to:

$$i \int_{-\infty}^{\infty} \frac{d\omega}{2\pi} \mathcal{G}(k)\mathcal{G}(-q_1 - q_2 - k)\mathcal{T}_2(-q_1 - k)\Phi(q_1, k) = - \frac{\mathcal{T}_2(-\xi_{\mathbf{q}_1} - \xi_{\mathbf{k}}, \mathbf{q}_1 + \mathbf{k})}{\xi_{\mathbf{q}_1} + \xi_{\mathbf{q}_2} + \xi_{\mathbf{k}} + \xi_{\mathbf{q}_1 + \mathbf{q}_2 + \mathbf{k}}} \Phi(\mathbf{q}_1, \mathbf{k}). \quad (\text{A2})$$

Here we denote  $\Phi(\mathbf{q}_1, \mathbf{q}_2) = \Phi(\{\mathbf{q}_1, \xi_{\mathbf{q}_1}\}, \{\mathbf{q}_2, \xi_{\mathbf{q}_2}\})$ .

The frequency integration of the third term in Eq.(A1) over the frequencies  $\Omega$  and  $\omega$  is more difficult because singularities are not essentially located in one half of the complex plane, as it was the case for the second term. For example  $\Phi(k, Q - k)$  has singularities in both half planes, with respect to  $\omega$ , and similarly for  $\mathcal{T}_2(-Q)\mathcal{T}_2(Q)$  with

respect to  $\Omega$ . We solve this problem by splitting the involved functions as the sum of two parts, one analytical in the upper complex plane, and the other one in the lower complex plane.

First we write  $F(\Omega, \mathbf{Q}, \mathbf{q}_1, \mathbf{q}_2) \equiv \mathcal{G}(Q - q_1)\mathcal{G}(-Q - q_2)\mathcal{T}_2(-Q)\mathcal{T}_2(Q) + (q_1 \leftrightarrow q_2)$  (we take into account that we want to calculate  $\Phi(q_1, q_2)$  "on the shell") as:

$$F(\Omega, \mathbf{Q}, \mathbf{q}_1, \mathbf{q}_2) = U_+(\Omega, \mathbf{Q}, \mathbf{q}_1, \mathbf{q}_2) + U_-(\Omega, \mathbf{Q}, \mathbf{q}_1, \mathbf{q}_2) \quad (\text{A3})$$

where  $U_+$  and  $U_-$  are respectively analytical in the upper and lower complex planes of  $\Omega$ . This is done by making use of the Cauchy formula  $f(\Omega) = (1/2i\pi) \int_C dz f(z)/(z - \Omega)$  for a contour  $C$  which encircles the real axis (on which  $F$  has no singularity) and is infinitesimally near of it. This gives:

$$U_+(\Omega, \mathbf{Q}, \mathbf{q}_1, \mathbf{q}_2) = \frac{1}{2i\pi} \int_{-\infty}^{\infty} dz \frac{F(z, \mathbf{Q}, \mathbf{q}_1, \mathbf{q}_2)}{z - i\epsilon - \Omega} \quad (\text{A4})$$

with  $\epsilon = 0_+$ . Making use of  $F(-\Omega) = F(\Omega)$ , we find  $U_-(\Omega, \mathbf{Q}, \mathbf{q}_1, \mathbf{q}_2) = U_+(-\Omega, \mathbf{Q}, \mathbf{q}_1, \mathbf{q}_2)$ .

On the other hand the last part of the third term  $\bar{T}_4(Q') \equiv \int d^4k' \mathcal{G}(k')\mathcal{G}(Q' - k')\Phi(k', Q' - k') = \int d^4k' \mathcal{G}(Q'/2 + k')\mathcal{G}(Q'/2 - k')\Phi(Q'/2 + k', Q'/2 - k')$  satisfies  $\bar{T}_4(-Q') = T_4(Q')$ . This can be seen by substituting Eq.(A1) for  $\Phi(Q'/2 + k', Q'/2 - k')$  in this last expression for  $\bar{T}_4(Q')$ . For the first term contribution, the result is trivial. For the second term, one has to make the shift  $k \rightarrow k - Q'/2$ , and then  $k \leftrightarrow k'$ . In the third term one has to make the shift  $k' \rightarrow k' + Q'/2$  and then  $k' \rightarrow -k'$ . Then, when we make the change  $Q \rightarrow -Q$  in the third term of Eq.(A1) and use  $\bar{T}_4(-Q) = T_4(Q)$ , we see that the  $U_-$  contribution is exactly identical to the  $U_+$  contribution and we are left with a single contribution from  $U_-$  to evaluate.

In order to perform the  $\omega$  integration in  $\bar{T}_4(Q) = \int d^4k \mathcal{G}(Q/2 + k)\mathcal{G}(Q/2 - k)\Phi(Q/2 + k, Q/2 - k)$ , we split:

$$\Phi(Q/2 + k, Q/2 - k) = \Phi_+(Q/2 + k, Q/2 - k) + \Phi_-(Q/2 + k, Q/2 - k) \quad (\text{A5})$$

into the sum of two functions, with  $\Phi_+$  analytical in the upper complex plane with respect to  $\omega$ , and  $\Phi_-$  analytical in the lower complex plane. That this can be done is immediately seen from Eq.(A1) itself. For the first term we just have to write the product of Green's functions as  $\mathcal{G}(k - Q/2)\mathcal{G}(-k - Q/2) = -(\mathcal{G}(k - Q/2) + \mathcal{G}(-k - Q/2))/(\Omega + \xi_{\mathbf{k} + \mathbf{Q}/2 + \xi_{\mathbf{k} - \mathbf{Q}/2} - i\epsilon)$ , which has explicitly the required property. In the third term we can handle the product of the first two Green's functions in the same way. Finally, in the second term, after performing the  $\omega$  integration as indicated above (but without taking the "on the shell" values for the frequencies), one sees that the result for the term written explicitly above in Eq.(A1) is analytical in the lower complex plane with respect to  $\omega$ . The corresponding term obtained by  $(q_1 \leftrightarrow q_2)$  is analytical in the upper complex plane. In each case one checks that the functions analytical in the upper and lower complex plane are related by  $k \leftrightarrow -k$ , so that  $\Phi_-(Q/2 + k, Q/2 - k) = \Phi_+(Q/2 - k, Q/2 + k)$ . Hence by the change of variable  $k \leftrightarrow -k$ , the contributions of  $\Phi_+$  and  $\Phi_-$  are equal.

Then we have arrived, for the calculation of  $\bar{T}_4(Q)$ , to a situation which is similar to the one we met for three particles. Since  $\Phi_+(Q/2 - k, Q/2 + k)$  and  $\mathcal{G}(Q/2 - k)$  are analytical in the lower complex plane, we can close the integration contour at infinity in this lower half plane and the only contribution comes from the pole of  $\mathcal{G}(Q/2 + k)$ . This leads to:

$$\bar{T}_4(Q) = -2i \int \frac{d\mathbf{k}}{(2\pi)^3} \frac{\mathcal{F}(\Omega, \mathbf{k}, \mathbf{Q})}{\Omega - \xi_{\mathbf{k} + \mathbf{Q}/2} - \xi_{\mathbf{k} - \mathbf{Q}/2} + i\epsilon} \quad (\text{A6})$$

where  $\mathcal{F}(\Omega, \mathbf{k}, \mathbf{Q})$  is  $\Phi_+(Q/2 - k, Q/2 + k)$  evaluated for  $\omega = \xi_{\mathbf{k} + \mathbf{Q}/2} - \Omega/2$ . An important property, which can be checked on each term contributing to  $\Phi_+(Q/2 - k, Q/2 + k)$  is that  $\mathcal{F}(\Omega, \mathbf{k}, \mathbf{Q})$  is analytical in the lower complex plane with respect to  $\Omega$ . Hence the integration of  $U_-(\Omega, \mathbf{Q}, \mathbf{q}_1, \mathbf{q}_2)\bar{T}_4(Q)$  over  $\Omega$  can also be performed by closing the contour in the lower half plane, since the only singularity in this half plane is the pole due to the denominator in Eq.(A6). The contribution of this pole leads to the evaluation of  $\mathcal{F}(\Omega, \mathbf{k}, \mathbf{Q})$  for  $\Omega = \xi_{\mathbf{k} + \mathbf{Q}/2} + \xi_{\mathbf{k} - \mathbf{Q}/2}$ . Taken with the above definition of  $\mathcal{F}$  this means that we have calculated  $\Phi_+(Q/2 - k, Q/2 + k)$  for  $\Omega/2 - \omega = \xi_{\mathbf{k} - \mathbf{Q}/2}$  and  $\Omega/2 + \omega = \xi_{\mathbf{k} + \mathbf{Q}/2}$ , which is just an evaluation "on the shell". Because of the simple relation between  $\Phi_+$  and  $\Phi_-$  the result can be expressed in terms of  $\Phi(\mathbf{k} + \mathbf{Q}/2, -\mathbf{k} + \mathbf{Q}/2)$  itself.

Gathering all the above results we end up with the following complete equation for  $\Phi(\mathbf{q}_1, \mathbf{q}_2)$ :

$$\begin{aligned} \Phi(\mathbf{q}_1, \mathbf{q}_2) = & -\frac{1}{4\xi_{\mathbf{q}_1}\xi_{\mathbf{q}_2}} + \int \frac{d^3\mathbf{k}}{(2\pi)^3} \frac{\mathcal{T}_2(-\xi_{\mathbf{q}_1} - \xi_{\mathbf{k}}, \mathbf{q}_1 + \mathbf{k})}{\xi_{\mathbf{q}_1} + \xi_{\mathbf{q}_2} + \xi_{\mathbf{k}} + \xi_{\mathbf{q}_1 + \mathbf{q}_2 + \mathbf{k}}} \Phi(\mathbf{q}_1, \mathbf{k}) \\ & - \int \frac{d^3\mathbf{Q}}{(2\pi)^3} \frac{d^3\mathbf{k}}{(2\pi)^3} U(\xi_{\mathbf{k} + \mathbf{Q}/2} + \xi_{\mathbf{k} - \mathbf{Q}/2}, \mathbf{Q}, \mathbf{q}_1, \mathbf{q}_2) \Phi(\mathbf{k} + \mathbf{Q}/2, -\mathbf{k} + \mathbf{Q}/2) + (q_1 \leftrightarrow q_2). \quad (\text{A7}) \end{aligned}$$

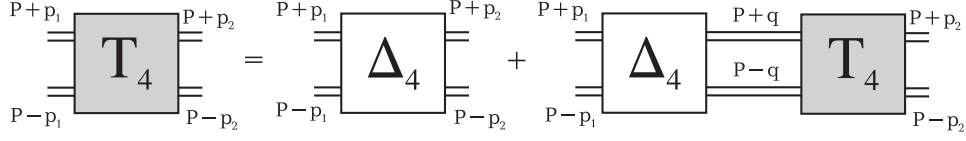


FIG. 9: The diagrammatic representation of the equation for the full dimer-dimer scattering vertex  $T_4(p_1, p_2; P)$ .

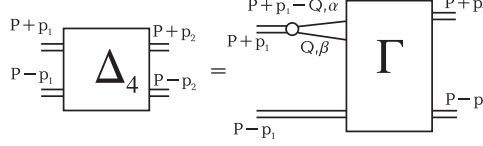


FIG. 10: The diagrammatic representation of the sum of all irreducible diagrams  $\Delta_4(p_1, p_2; P)$ .

In this equation we have modified the integration contour in the definition of  $U_-$  to have it running on the imaginary axis rather than on the real axis, and we have used the symmetry property of  $F(z, \mathbf{Q}, \mathbf{q}_1, \mathbf{q}_2)$  with respect to  $z$ , together with symmetry properties of  $\Phi(\mathbf{q}_1, \mathbf{q}_2)$ , to rewrite the result in terms of the real function:

$$U(\Omega, \mathbf{Q}, \mathbf{q}_1, \mathbf{q}_2) = \frac{\Omega}{\pi} \int_0^\infty dy \frac{F(iy, \mathbf{Q}, \mathbf{q}_1, \mathbf{q}_2)}{y^2 + \Omega^2} \quad (\text{A8})$$

which shows that  $\Phi(\mathbf{q}_1, \mathbf{q}_2)$  itself is real.

We have made practical numerical use of Eq. (A7) to find for example the ground state energy. Although this turned out to be quite feasible, this equation appears finally less convenient than what we have described in section IV. This was expected since the solution implies quadruple integrals, instead of the triple integrals we had only to deal with in section IV.

## APPENDIX B: MODIFIED DIMER-DIMER SCATTERING EQUATION

This appendix is devoted to an alternative description of the dimer-dimer scattering process. The purpose is to obtain a direct integral equation for  $T_4(p_1, p_2; P)$ , in a way convenient for numerical calculations. Below we derive such a set of equations, that were used for practical computations as indicated in section IV.

The first step is to construct for two dimers a "bare" interaction potential, or vertex,  $\Delta_4$ , which is the sum of all irreducible diagrams, and then to build ladder diagrams from this vertex, in order to obtain an integral equation (see Fig. 9). These irreducible diagrams are those ones which cannot be divided by a vertical line into two parts connected by two dimer lines. As it was pointed above the vertex  $\Delta_4$  is given by the series shown on Fig.4e, since the diagrams on Fig.4f are by contrast reducible. Again we can eliminate  $T_3$  from our considerations and express  $\Delta_4$  only in terms of  $T_2$ . For this purpose we have to introduce a special vertex with two fermionic and one dimer incoming lines and two dimer outgoing lines  $\Gamma_{\alpha\beta}(q_1, q_2; p_2, P)$  (see Fig. 10). This vertex  $\Gamma_{\alpha\beta}(q_1, q_2; p_2, P)$  corresponds to the vertex  $\Delta_4$  with one incoming dimer line being removed, in much the same way as  $\Phi(q_1, q_2; p_2, P)$  and  $T_4(p_1, p_2; P)$  are related in Eq. (8). The difference is that  $\Gamma_{\alpha\beta}(q_1, q_2; p_2, P)$  is irreducible with respect to two dimer lines while  $\Phi(q_1, q_2; p_2, P)$  is not, just in the same way as  $T_4(p_1, p_2; P)$  and  $\Delta_4(p_1, p_2; P)$  are related. The corresponding equation relating  $\Gamma_{\alpha\beta}(q_1, q_2; p_2, P)$  and  $\Delta_4(p_1, p_2; P)$  is:

$$\Delta_4(p_1, p_2; P) = \frac{1}{2} \sum_{Q; \alpha, \beta} \chi(\alpha, \beta) G(P + p_1 - Q) G(Q) \Gamma_{\alpha\beta}(P + p_1 - Q, Q; p_2, P). \quad (\text{B1})$$

One can readily verify that the diagrammatic expansion for  $\Gamma$  shown on Fig. 11 yields the same series as the one shown on Fig. 4e for the vertex  $\Delta_4$ . The spin part of  $\Gamma_{\alpha, \beta}$  has again the simple form  $\Gamma_{\alpha, \beta}(q_1, q_2; P, p_2) = \chi(\alpha, \beta) \Gamma(q_1, q_2; p_2, P)$  and the function  $\Gamma(q_1, q_2; p_2, P)$  obeys the following equation:

$$\Gamma(q_1, q_2; p_2, P) = -G(P - q_1 + p_2) G(P - q_2 - p_2) - G(P - q_2 + p_2) G(P - q_1 - p_2) - \sum_Q G(Q) G(2P - q_1 - q_2 - Q) [T_2(2P - q_1 - Q) \Gamma(q_1, Q; p_2, P) + T_2(2P - q_2 - Q) \Gamma(Q, q_2; p_2, P)]. \quad (\text{B2})$$

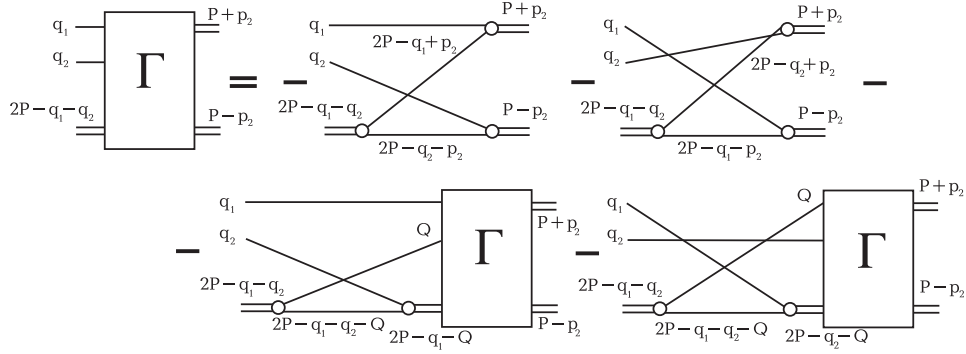


FIG. 11: The graphic representation of the equation on the full vertex  $\Gamma(q_1, q_2; p_2, P)$ .

The sign minus in (B2) is a consequence of the anticommutativity of Fermi operators. It is clear that Eqs. (B1) and (B2) can be analytically integrated over the variable  $\Omega$ . Thus the  $s$ -wave component of the vertex  $\Gamma(q_1, q_2; p_2, P)$  is a function of the absolute values of vectors  $|\mathbf{q}_1|$  and  $|\mathbf{q}_2|$ , the angle between them, the absolute value of vector  $|\mathbf{p}_2|$ , and the frequency  $\omega_2$ . The  $s$ -wave component of the sum of all irreducible diagrams  $\Delta_4(p_1, p_2; P)$  is a function of the absolute values of the vectors  $|\mathbf{p}_1|$  and  $|\mathbf{p}_2|$  and the frequencies  $\omega_1$  and  $\omega_2$ .

The fully symmetrized vertex  $T_4(p_1, p_2; P)$  of two-dimer scattering can be found from the solution of the following equation (see Fig. 9):

$$T_4(p_1, p_2; P) = \Delta_4(p_1, p_2; P) + \frac{1}{2} \sum_q \Delta_4(p_1, q; P) T_2(P+q) T_2(P-q) T_4(q, p_2; P), \quad (\text{B3})$$

where  $\Delta_4(p_1, p_2; P)$  is the sum of all irreducible diagrams,  $P \pm p_{1,2} = \{-E_b \pm \omega_{1,2}, \pm \mathbf{p}_{1,2}\}$  are 4-vectors of incoming (1) and outgoing (2) dimers in the center-of-mass system.

Let us finally note that, equivalently to our above derivation, Eq. (B1-B3) can be also related to Eq. (8) and Eq. (9) algebraically by simple formal operator manipulations.

## ACKNOWLEDGMENTS

This work was supported by Russian Foundation for Basic Research (Grant No. 04-02-16050), CRDF (Grant No. RP2-2355-MO-02) and the grant of Russian Ministry of Science and Education. We are grateful to A.F. Andreev, I.A. Fomin, P. Fulde, Yu. Kagan, L.V. Keldysh, Yu. Lozovik, S.V. Maleev, B.E. Meierovich, A.Ya. Parshin, P. Pieri T.M. Rice, V.N. Ryzhov, G.V. Shlyapnikov, G.C. Strinati, V.B. Timofeev, D. Vollhardt and P. Wölfle for fruitful discussions. M.Yu.K is grateful to the University Pierre and Marie Curie for the hospitality on the first stage of this work.

Laboratoire de Physique Statistique is " Laboratoire associé au Centre National de la Recherche Scientifique et aux Universités Paris 6 et Paris 7 ".

\* Corresponding author: kagan@kapitza.ras.ru

<sup>1</sup> *Workshop on ultracold fermi gases* (2004), (Levico), <http://bec.science.unitn.it/fermi04/>.

<sup>2</sup> M. Greiner, C. Regal, and D. Jin, *Nature* **426**, 537 (2003).

<sup>3</sup> S. Jochim, M. Bartenstein, A. Altmeyer, G. Hendl, S. Riedl, C. Chin, J. H. Denschlag, and R. Grimm, *Science* **302**, 2101 (2003).

<sup>4</sup> M. W. Zwierlein, C. A. Stan, C. H. Schunck, S. M. F. Raupach, S. Gupta, Z. Hadzibabic, and W. Ketterle, *Phys. Rev. Lett.* **91**, 250401 (2003).

<sup>5</sup> T. Bourdel, L. Khaykovich, J. Cubizolles, J. Zhang, F. Chevy, M. Teichmann, L. Tarruell, S. J. J. M. F. Kokkelmans, and C. Salomon, *Phys. Rev. Lett.* **93**, 050401 (2004).

<sup>6</sup> G. V. Skorniakov and K. A. Ter-Martirosian, *Zh. Eksp. Teor. Phys* **31**, 775 (1956), [*Sov. Phys. - JETP* **4**, 648 (1957)].

<sup>7</sup> R. Haussmann, *Z. Phys. B: Condens. Matter* **91**, 291 (1993).

<sup>8</sup> P. Pieri and G. C. Strinati, *Phys. Rev. B* **61**, 15370 (2000).

<sup>9</sup> D. S. Petrov, C. Salomon, and G. V. Shlyapnikov, *Phys. Rev. Lett.* **93**, 090404 (2004).

- <sup>10</sup> D. S. Petrov, C. Salomon, and G. V. Shlyapnikov, Phys. Rev. A **71**, 012708 (2005).
- <sup>11</sup> M. Yu. Kagan and T. M. Rice, J.Phys.: Condens. Matter **6**, 3771 (1994).
- <sup>12</sup> M. Yu. Kagan, R. Fresard, M. Capezzali, and H. Beck, Phys. Rev. B **57**, 5995 (1998).
- <sup>13</sup> M. Yu. Kagan and D. V. Efremov, Phys. Rev. B **65**, 195103 (2002).
- <sup>14</sup> M. Yu. Kagan, I. V. Brodsky, D. V. Efremov, and A. V. Klaptsov, Phys. Rev. A **70**, 023607 (2004).
- <sup>15</sup> P. F. Bedaque and U. van Kolck, Phys. Lett. B **428**, 221 (1998).
- <sup>16</sup> S. Weinberg, Phys. Rev **133**, B232 (1964).
- <sup>17</sup> D. S. Petrov, M. A. Baranov, and G. V. Shlyapnikov, Phys. Rev. A. **67**, 031601(R) (2003).
- <sup>18</sup> V. N. Popov, Zh. Eksp. Teor. Phys **50**, 1550 (1966), [Sov. Phys. - JETP **23**, 1034 (1966)].
- <sup>19</sup> L. V. Keldysh and A. N. Kozlov, Zh. Eksp. Teor. Phys **54**, 978 (1968), [Sov. Phys. - JETP **27**, 521 (1968)].
- <sup>20</sup> W. H. Press, S. A. Teukolsky, W. T. Vetterling, and B. P. Flannery, *Numerical Recipes: The Art of Scientific Computing* (Cambridge University Press, Cambridge, 1996).
- <sup>21</sup> G. S. Danilov, Zh. Eksp. Teor. Phys **40**, 498 (1961), [Sov. Phys. - JETP **13**, 349 (1961)].
- <sup>22</sup> R. Minlos and L. D. Fadeev, Zh. Eksp. Teor. Phys **41**, 1850 (1961), [Sov. Phys. - JETP **14**, 1315 (1962)].
- <sup>23</sup> L. W. Bruch and J. A. Tjon, Phys. Rev. A **19**, 425 (1979).
- <sup>24</sup> A. S. Jensen, K. Riisager, D. V. Fedorov, and E. Garrido, Rev. Mod. Phys. **76**, 215 (2004).
- <sup>25</sup> L. Platter, H. Hammer, and U. Meißner, Few Body Syst. **35**, 169 (2004), [cond-mat/0405660].
- <sup>26</sup> H. Hammer and D. T. Son, Phys.Rev.Lett. **93**, 250408 (2004).